

# Approximations and modifications of celestial dynamics tested on the three-body system

Søren Toxvaerd

*Department of Science and Environment, Roskilde University,*

*Postbox 260, DK-4000 Roskilde, Denmark\**

## Abstract

Large-scale simulations of celestial systems are based on approximations or modifications of classical dynamics. The approximations are with “particle-mesh” (PM) substitutions of the attractions from objects far away, or one modify the Newtonian accelerations (MOND) or the gravities (MOGA). The PM approximation and MOND modification of classical dynamics break the invariances of classical dynamics. The simple three-body system (TBS) is the simplest system to test the approximations and modifications of celestial dynamics, and it is easy to implement on a computer. Simulations of the TBS show that the PM approximation and MOND destabilize TBS. In contrast, the MOGA modification of gravity by replacing Newton’s inverse square attraction with an inverse attraction for far-away interactions stabilizes the system. The PM approximation and the MOND modification of classical dynamics do not preserve the momentum and angular momentum of a conservative system exactly, and PM does not obey Newton’s third law. Although the errors and shortcomings of these PM approximations and MOND modifications are small, they cause the instability of the regular dynamics.

---

\* st@ruc.dk

## I. INTRODUCTION

The time evolution of astronomical systems is obtained by simulations, where the objects' positions are calculated employing algorithms for discrete dynamics. This approach has been used since Newton's time, and today, the dynamics of galaxies with billions of suns are obtained by large-scale simulations. An overview of simulations of galaxial systems is given in [1, 2]. But the dynamic behavior of these large-scale simulations is achieved by making "particle-mesh" approximations (PM), PM3 [3, 4] or Tree-PM [5], for the small effects of the many objects that are far away and which are assumed to have only a minor influence on an object's motion. However, recent simulations indicate that the approximations used in the simulations destabilize the systems [6]. Here we investigate the approximation's impact on the stability of a regular dynamic in the simple "three-body system" (TBS).

The TBS has challenged science ever since Newton formulated classical mechanics in 1687, and simultaneously solved the dynamics of two celestial bodies [7]. Newton's solution of the dynamics of the two-body system satisfies Kepler's three laws for the planets in the solar system. Since the planets in the Solar system move in orbits, bound rotations must be a classical mechanical solution for a system with three as well as many celestial bodies. But although one cannot solve the coupled second-order differential equations, even for just a TBS, regular solutions have been found for the system [8–10]. An overview of the history of the three-body system and its dynamic behavior is given in [11], and how to simulate a TBS system are given in the Appendix.

Simulations of systems with classical dynamics are performed using discrete algorithms, and almost all simulations are with Newton's discrete algorithm [7, 12]. The classical dynamics obtained with this algorithm is time-reversible and symplectic, and has the same invariances (momentum, angular momentum, and energy) as the analytic dynamics. Hence, it is exact in the same sense as the corresponding exact solution to the coupled second-order differential equations for Newton's analytic dynamics [12–14]. Here, the exact discrete dynamics for TBS are used to investigate the sensitivities of the regular orbits to the various approximations and modifications used in large-scale simulations of celestial systems' dynamics.

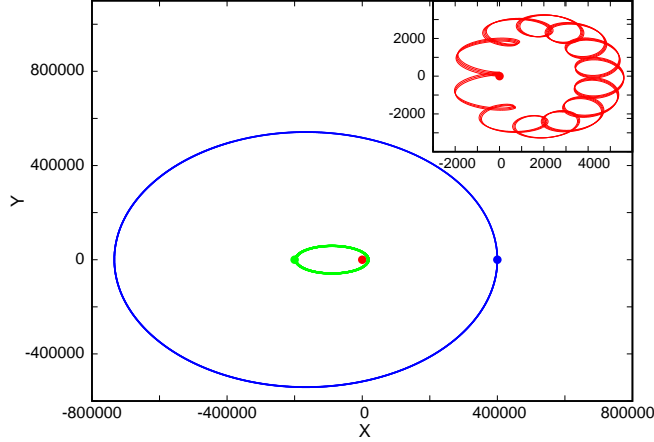


FIG. 1: The regular orbits in a TBS system with two light objects around a heavy object, and for  $10^7$  discrete timesteps. The  $\approx 45$  orbits in green is for the object No. 1 with start position at its aphelion (green dot), and with blue is the corresponding  $\approx$  four orbits for the object No. 2 with start position at its perihelion (blue dot). The red “dot” is the orbits of the heavy object No. 3 with start position at the center of mass (origin), and the inset shows the  $\approx$  four orbits of the object.

## II. THE DYNAMICS OF A THREE-BODY SYSTEM

Newtonian dynamics for celestial objects is given by Newton’s classical dynamics and his inverse-square law (ISL) of gravitation

$$\mathbf{F}_i(t) = m_i \mathbf{a}_i(t) = \sum_{j \neq i}^N \mathbf{f}_{ij}(t) = - \sum_{j \neq i}^N \frac{G m_i m_j}{r_{ij}^2(t)} \hat{\mathbf{r}}_{ij}(t) \quad (1)$$

for the acceleration  $\mathbf{a}_i(t) = \ddot{\mathbf{a}}_i(t)$  caused by the sum of forces  $\sum_{j \neq i}^N \mathbf{f}_{ij}(t)$  on the object  $i$  in the ensemble of  $N$  objects, by baryonic objects  $j$  with mass  $m_j$  at distances  $r_{ij}(t)$ , and at time  $t$ .

Newton’s discrete dynamics for TBS and how to start the TBS are described in the Appendix. The TBS can have solutions with regular orbits of the objects around their center of gravity. Here we want to set up a TBS with a heavy “sun” or mass center in a galaxy with two planets or stars in a galaxy, one inner and one outer object in the TBS. The TBS system with the ellipses in Figure 1 is with (mass in units of objects’ No. 1 mass, and dynamics units given by the gravitational constant  $G = 1$ ):  $m_1 = 1, m_2=0.5$  and  $m_3=100$ , and with the start position of No. 1 at  $[x_1(0), y_1(0)] = [-200000, 0]$ , No. 2 at  $[x_2(0), y_2(0)] = [400000, 0]$ ,

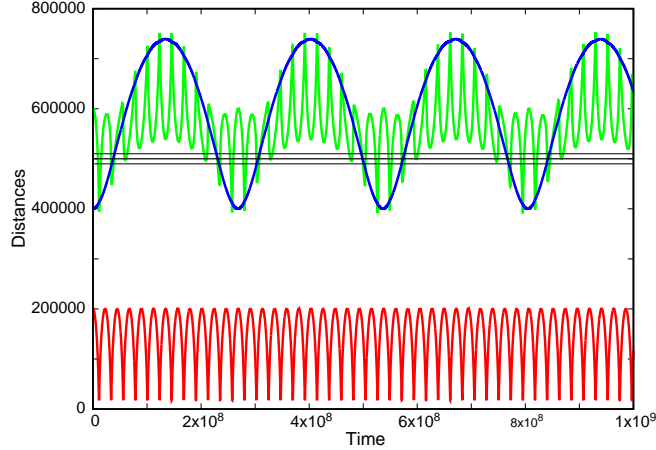


FIG. 2: The distances  $r_{12}(t)$  (green),  $r_{13}(t)$  (red), and  $r_{23}(t)$  (blue) between the three objects as a function of time for the regular orbits, shown in Figure 1. The thick black straight line is the borderline for the PM approximation,  $r_0=500000$ , and the thinn black lines are  $r_0 \pm l_{grid}$  with  $l_{grid}=10000$ , used in the PM approximation.

and with the heavy object at the origin at the start  $[x_3(0), y_3(0)] = [0, 0]$ . The orbits in the figure are obtained for  $10^7$  time steps with  $\delta t=100$  where object No. 1 in green had circulated  $\approx 45$  times in the elliptical orbit. In blue is the corresponding  $\approx$  four orbits of the light object No. 2, and the inset shows the heavy object's more complicated four orbits in red. The TBS was simulated  $10^{10}$  time steps, and the regular dynamics is stable.

The TBS is used for testing the stability of the system when exposed to the approximations and modifications of celestial dynamics.

### III. APPROXIMATIONS AND MODIFICATIONS OF CELESTIAL DYNAMICS

#### A. PM approximation of far-away interactions in the three-body system

In large-scale simulations of galaxies, one sorts the N-1 forces on object  $i$  in Eq. (1) into a sum of  $N'_i(t)$  short-range forces  $\mathbf{f}_{ij}(r_{ij})$  with distances  $r_{ij}(t)$ , which are less than a certain (large) distance  $r_0$ , and for which the forces are computed directly, and  $N''_i(t)$  forces from objects far away with  $r_{ij}(t) > r_0$ . Their positions are interpolated onto a mesh with a certain grid length  $l_{grid}$ , and their forces are taken from the centers  $\mathbf{r}_{\alpha(j)}(t)$  of the boxes  $\alpha(j)$ , with grid length  $l_{grid}$  and with a distance  $r_{i\alpha(j)}(t)$  and direction  $\hat{\mathbf{r}}_{i\alpha(j)}(t)$  to object  $i$ . The force on

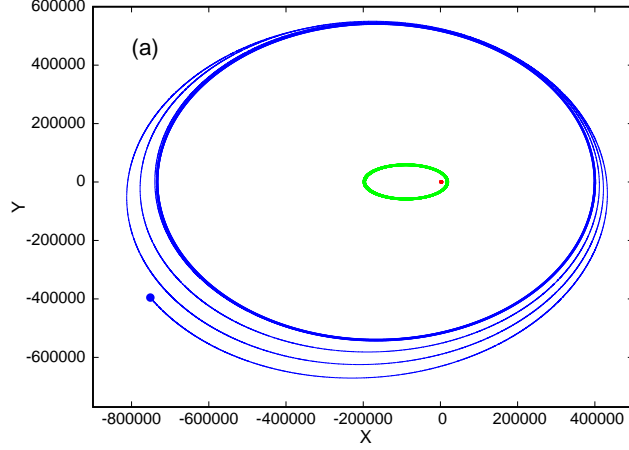


FIG. 3: The dynamics of TBS with the PM approximation with  $r_0 = 500000$  and  $l_{grid}=10000$ . The orbits are for  $10^7$  timesteps. The blue orbits are for No. 2. The thick blue ellipse is without PM approximation (also shown in Figure 1), and the orbits with thin blue are with the PM approximation. No. 1's orbits are in green with or without PM (the differences are not visible on the figures).

object  $j$  from  $i$  is correspondingly taken from the center  $\mathbf{r}_{\alpha(i)}(t)$  of the subbox with object  $i$ .

The division of the space into a sum of cubes with mean field attractions to  $i$  has the consequence that

$$r_{i\alpha(j)}(t) \neq r_{\alpha(i)j}(t) \neq r_{ij}(t) \quad (2)$$

$$\hat{\mathbf{r}}_{i\alpha(j)}(t) \cdot \hat{\mathbf{r}}_{j\alpha(i)}(t) \neq -1, \quad (3)$$

and

$$\mathbf{f}_{i\alpha(j)}(t) \neq -\mathbf{f}_{j\alpha(i)}(t) \neq \mathbf{f}_{ij}(t). \quad (4)$$

Eqn.(2)-(3) with  $0 \ll r_0$  and with the size length  $l_{grid} \ll r_0$  looks like excellent approximations. But it has the consequence that the symmetry of pair interactions is broken and that Newton's third law

$$\mathbf{f}_{ij}(t) = -\mathbf{f}_{ji}(t) \quad (5)$$

is no longer strictly valid for dynamics with the PM approximation of the long-range forces. The momentum and angular momentum of the system are not exactly conserved, and PM might destabilise the regular dynamics in a celestial system [6].

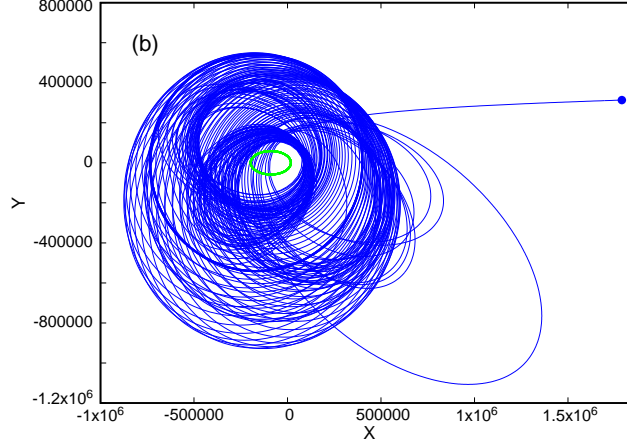


FIG. 4: The dynamics of TBS, also shown in Figure 3, but for  $1.49899436 \times 10^8$  timesteps with PM, and when No. 2 was released from the TBS.

The TBS system can be used to illustrate the destabilization of a celestial system by the PM approximation, and PM is easily implemented in TBS (see Appendix). PM primarily affects objects at distances in the outer edge of a celestial system and in the TBS system object no. 2. Figure 2 shows the distances  $r_{12}(t)$ ,  $r_{13}(t)$ , and  $r_{23}(t)$  for the regular orbits without PM, shown in Figure 1. With green and blue is  $r_{12}(t)$ ,  $r_{13}(t)$ , respectively, and  $r_{23}(t)$  is in red. The effect of a PM approximation on the regular dynamics of the TBS system, shown in Figure 1, is obtained for a far-away distance  $r_0 = 500000$  between two objects. The far-away distance is  $r_0 = 500000$ , marked by a solid line in Figure 2, and the thin solid lines are  $r_0 = 500000 \pm l_{grid}$  with  $l_{grid} = 10000$ . This PM choice affects the far-away object, No. 2's regular dynamics by changing the direction primarily, and a percent change in the distance on average. However, it is sufficient to disrupt the system's stability.

Figure 3 and Figure 4 illustrate the effect of the PM approximation with  $r_0 = 500000$  and  $l_{grid} = 10000$ . Figure 3 shows the PM effect for the first  $10^7$  time steps (the color of the orbits is the same as in Figure 1). The PM affects primarily object No. 2's regular dynamics (in blue), and the effect on object No. 1 (in green) and the heavy object No. 3 (in red) is not visible in the figures. Object No. 2 begins to perform “revolving orbits” by being exposed to the PM, and it is released from its regular dynamics after  $1.49899436 \times 10^8$  time steps (Figure 4). The PM effect was tested for many other choices of  $r_0$  and  $l_{grid}$ , and for other TBS systems. The destabilizing decreases with increasing  $r_0$  and decreasing grid

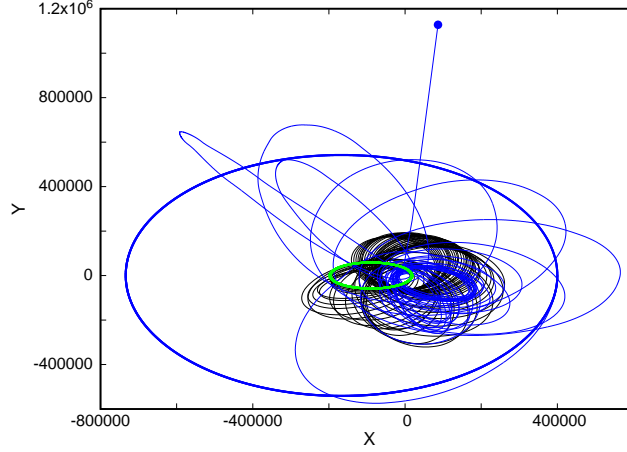


FIG. 5: The MOND modification for  $a_0 = 4 \times 10^{-12}$  (corresponding to  $r_0 = 500000$  in MOGA and PM). The orbits with MOND dynamics are shown in thin blue for No. 2, and in thin black for No. 1. The position of No. 2 at  $t = 1.2576 \times 10^9$  at its release is marked with a blue sphere. The ellipses with thick blue and green (from Fig. 1) are without MOND modification.

length  $l_{grid}$ . But even a small change of focus for the distance  $r_{12}$  and  $r_{13}$ , and direction of the forces  $\mathbf{f}_{12}(t)$  and  $\mathbf{f}_{23}(t)$  are sufficient to destroy object No's regular dynamics, as illustrated in Figure 4.

## B. MOND and MOGA modifications

Theoretically, one can modify the classical dynamics of a celestial system of  $N$  objects, with the acceleration  $\mathbf{a}_i$  and force  $\mathbf{F}_i$

$$\mathbf{a}_i(t) = \mathbf{F}_i(t)/m_i \quad (6)$$

in Eq. (1) in at least two ways: by modifying the accelerations  $\mathbf{a}_i(t)$ (MOND) [16] or by modifying the gravitational attractions  $\mathbf{F}_i(t)$  (MOGA) [18]. The two modifications are equal for a system of two objects [18], but they differ significantly for a many-body system.

The modification,  $\mu$  in MOND, of the acceleration  $|\mathbf{a}_i|$  is obtained with the "standard interpolation function"

$$\mu(a/a_0) = \sqrt{\frac{1}{1 + (\frac{a_0}{a})^2}}, \quad (7)$$

or the interpolation function proposed in [17]

$$\mu(a/a_0) = \frac{|a|}{|a| + a_0}, \quad (8)$$

with the MOND modification given by

$$\mathbf{F}_i/m_i = \mathbf{a}_i \frac{|\mathbf{a}_i|}{|\mathbf{a}_i| + a_0}, \quad (9)$$

and acceleration

$$\mathbf{a}_i(\text{MOND}) = \frac{\mathbf{F}_i}{2m_i} (1 + \sqrt{1 + 4m_i a_0 / |\mathbf{F}_i|}). \quad (10)$$

MOND does not conserve momentum and angular momentum of a gravitational system because

$$\mathbf{f}_{ij}(t) \sqrt{1 + 4m_i a_0 / |\mathbf{F}_i|} \neq -\mathbf{f}_{ji}(t) \sqrt{1 + 4m_j a_0 / |\mathbf{F}_j|}. \quad (11)$$

The modifications, Eq. (7) or Eq. (8), change the acceleration from the Newtonian acceleration for  $|\mathbf{a}_i| \gg a_0$  at short distances to a modified acceleration

$$|\mathbf{a}_i(\text{MOND})| = \sqrt{|\mathbf{F}_i| a_0 / m_i} \quad (12)$$

for  $|\mathbf{a}_i| \ll a_0$ .

The asymptotic modified acceleration for an isolated object  $i$  with only one gravitational interaction,  $|\mathbf{F}_i(r_{ij})| = -m_i m_j G / r_{ij}^2$ , with another object, No.  $j$ , is obtained from Eq. (1) and Eq.(10) as

$$|\mathbf{a}_i(\text{MOND})| = -\frac{\sqrt{m_j G a_0}}{r_{ij}}. \quad (13)$$

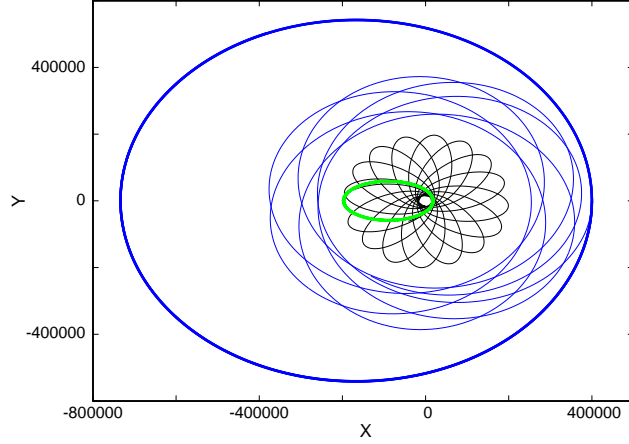
MOND is a modification of Newtonian acceleration. But in this case, the modification might as well be formulated as a modification of Newton's ISL law of universal gravitational attraction, where the inverse square attraction asymptotically is replaced with an inverse attraction (IA). If this modified gravitational attraction is a universal law, MOGA, the gravitational force is modified to

$$\mathbf{F}_i(\text{MOGA}) = -\sum_{j \neq i}^N \frac{m_i m_j G}{r_{ij}^2} \left(1 + \frac{r_{ij}}{r_0}\right) \hat{\mathbf{r}}_{ij}(t) \quad (14)$$

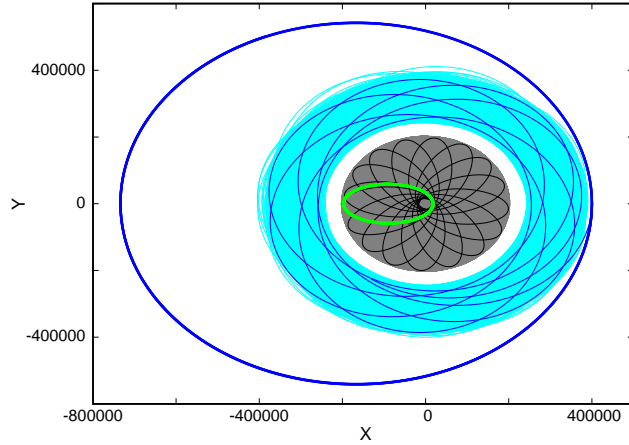
with  $r_0 = \sqrt{m_j G / a_0}$ .

The PM approximation (Figure 3 and Figure 4) is for distances  $r > r_0 = 500000$ , and the results for the dynamics with MOGA and MOND are correspondingly for  $r_0 = 500000$  (MOGA) and  $a_0 = r_0^{-2} = 4 \times 10^{-12}$  (MOND).





(a) The start of MOGA. The revolving elliptical orbits are shown in black for No.1 and blue for No. 2, together with the elliptical orbits without MOGA ( from Figure 1) with thick lines. The simulations are for the times where the elliptical orbits have revolved  $2\pi$  .



(b) The revolving orbits with MOGA and for  $10^9$  timesteps. The revolving elliptical orbits with gray for No. 1 and in light blue for No. 2 are shown together with the orbits from Figure 6(a).

FIG. 6: Simulation with MOGA and for  $r_0 = 500000$ .

Figure 5 shows the impact of MOND on the regular dynamics in the TBS. The orbits are for  $1.2576 \times 10^7$  time steps with  $\delta t = 100$ , and at the time where object No. 2 (in blue) is released from the TBS. But opporside the dynamics with PM also object No. 1 nearby the center of gravity is affected by the MOND modification of the acceleration. Its orbits are shown in black in the figure. Simulations with other values of  $a_0$  gave the same result. The regular dynamics in TBS are sensitive to the MOND modification of the acceleration and

with a breakdown of the regular dynamics and the release of the objects.

The corresponding impact of the MOGA modification of the attractions is shown in Figure 6. The dynamics are for the modification distance  $r_0 = 500000$ , as in PM and MOND. Opposite PM and MOND, the modification of the gravitational attractions from an inverse square attraction to an inverse attraction conserves the classical dynamics invariances, and MOGA stabilizes the regular dynamics, but with “revolving” elliptical orbits [19]. Figure 6(a) shows the orbits after the revolving orbits have turned  $2\pi$  around. For No.1 (in black) after  $t_1 = 3.155 \times 10^6$  timesteps, and after  $t_2 = 2 \times t_1 = 6.310 \times 10^6$  time steps for No. 2 (in thin blue). The revolving orbits are with conservation of the length of the principal axis. Figure 6 (b) shows the revolving orbits after  $10^9$  timesteps with the orbits of No. 1 in gray and light blue for No. 2.

The MOGA modification of Newton’s ISL to an inverse attraction for large interaction distance  $R$  is an example of the  $f(R)$  modification of gravity, introduced in the standard model [20–22]. Simulation of large-scale celestial systems with modified gravity is described in [23] and cosmological tests of modified gravity are reviewed in [24]. MOGA changes the rotation velocities from a Kepler-like behavior to a relatively constant rotation velocity in a galaxy, independent of the average distance to the galaxy center, and qualitatively consistent with the experimental data [18]. In [18], we suggested that the modification of the ISL attractions is caused by lensing by the gravitational objects in the central part of the galaxy, of the interactions from far-away objects. A lensing that will act as a self-stabilizing effect on the halos in the galaxies.

#### IV. CONCLUSION

The three-body system (TBS) is the simplest celestial system to test the approximations and modifications used in celestial dynamics, and it is easy to implement on a computer (see Appendix). The simulations of TBS without PM approximations or MOND modifications, acknowledging all the symmetry requirements and dynamical invariances in classical mechanics, show that the regular dynamics are stable, but that the PM approximation and MOND modification destabilise TBS. In contrast, the modified gravity (MOGA) of Newton’s inverse square attraction to an inverse attraction stabilises the system.

Classical dynamics for an  $N$ -body system have regular stable orbits, but this property is

sensitive to violations of the invariances in Newtonian dynamics [14]. The stability of a TBS system for other values of masses of the objects, and PM modifications  $r_0$  and  $l_{grid}$  exhibited the same qualitative behaviour with a destabilisation of the regular dynamics. However, an extrapolation from a three-body system to a galaxy with a hundred billion stars must be taken cautiously, and only additional simulations can reveal the stability of galaxies with and without approximations. But large-scale simulations without PM approximation are extremely time-demanding.

## V. ACKNOWLEDGMENT

This work was supported by the VILLUM Foundation’s Matter project, grant No. 16515.

**Data availability**— Data and computer programs will be available on request.

## VI. APPENDIX

### A. Newton’s Discrete algorithm

Almost all simulations of celestial systems are with Newton’s algorithm for discrete dynamics. In Newton’s discrete dynamics [7] the time and forces are discrete with discrete force impulses at every discrete times  $t, t + \delta t, t + 2\delta t, \dots$ . A new position  $\mathbf{r}_i(t + \delta t)$  at time  $t + \delta t$  of an object  $i$  with the mass  $m_i$  is determined by the force impulse  $\mathbf{f}_i(t)$  at time  $t$  acting on the object at the positions  $\mathbf{r}_i(t)$ , and the position  $\mathbf{r}_i(t - \delta t)$  at  $t - \delta t$  as

$$m_i \frac{\mathbf{r}_i(t + \delta t) - \mathbf{r}_i(t)}{\delta t} = m_i \frac{\mathbf{r}_i(t) - \mathbf{r}_i(t - \delta t)}{\delta t} + \delta t \mathbf{f}_i(t), \quad (15)$$

where the momenta  $\mathbf{p}_i(t + \delta t/2) = m_i(\mathbf{r}_i(t + \delta t) - \mathbf{r}_i(t))/\delta t$  and  $\mathbf{p}_i(t - \delta t/2) = m_i(\mathbf{r}_i(t) - \mathbf{r}_i(t - \delta t))/\delta t$  are constant in the time intervals in between the discrete positions.

Usually, the algorithm, Eq. (1), is presented as the Leap-frog algorithm for the velocities

$$\mathbf{v}_i(t + \delta t/2) = \mathbf{v}_i(t - \delta t/2) + \delta t/m_i \mathbf{f}_i(t), \quad (16)$$

and the positions are determined from the discrete values of the momenta/velocities as

$$\mathbf{r}_i(t + \delta t) = \mathbf{r}_i(t) + \delta t \mathbf{v}_i(t + \delta t/2). \quad (17)$$

The discrete algorithm is time-reversible due to the time symmetry, which also ensures the symplecticity and the energy conservation [12], and Newton's third law

$$\mathbf{f}_{ij}(t) = -\mathbf{f}_{ji}(t) \quad (18)$$

ensures the conservation of momentum and angular momentum.

## B. The three-body system

The TBS consists of three objects with masses  $m_1, m_2$ , and  $m_3$ . The Newtonian discrete dynamics with time increment  $\delta t$  is obtained from three positions  $\mathbf{r}_1(t), \mathbf{r}_2(t)$ , and  $\mathbf{r}_3(t)$  and three velocities  $\mathbf{v}_1(t - \delta t/2), \mathbf{v}_2(t - \delta t/2)$ , and  $\mathbf{v}_3(t - \delta t/2)$ , in total six three-dimensional dynamic variables. The present TBS is started at time  $t = 0$  with all three objects in their aphelion or perihelion and with start velocities in the “Ècliptica” plane, given by the plane with the three objects' positions at the start. The three objects remain in the plane since the discrete dynamics conserves momentum, and the system is two-dimensional (2D), and with three (x,y)-positions and their velocities, in total, twelve dynamic values which need to be specified at the start of the simulation. The conserved momentum and center of mass reduces the number of necessary start values to eight.

The TBS exhibits a variety of regular dynamics depending on the start values, for a review see [11]. The present TPS system is created with two objects in elliptical orbits around a third heavy object. The objects' six components of position  $x_1(0), y_1(0), x_2(0), y_2(0), x_3(0), y_3(0)$  and six velocity components  $vx_1(-\delta t/2), vy_1(-\delta t/2), vx_2(-\delta t/2), vy_2(-\delta t/2), vx_3(-\delta t/2), vy_3(-\delta t/2)$  must be specified.

Aphelion or perihelion, with the longest of the principal axes in the x-direction, determines six start values:

$$y_1(0) = y_2(0) = y_3(0) = 0, \quad (19)$$

and with

$$vx_1(0) = vx_2(0) = vx_3(0) = 0. \quad (20)$$

We need to know the velocities, not at time  $t = 0$ , but at time  $-\delta t/2$ . However, these velocities can be calculated by the algorithm and the force in the x-direction  $\mathbf{f}_x(0)$  using

time symmetry since

$$vx_1(\delta t/2) = -vx_1(-\delta t/2) \text{ (time reversibility)}, \quad (21)$$

and (Eq. 16)

$$vx_1(\delta t/2) = vx_1(-\delta t/2) + \delta t/m_1 \mathbf{f}_{x_1}(0), \quad (22)$$

by which

$$vx_1(-\delta t/2) = -\delta t \mathbf{f}_{x_1}(0)/2m_1, \quad (23)$$

and correspondingly for the two other objects.

The conserved momentum and center of mass give two relations. Let the conserved center of mass be the origin of the 2D coordinate system, then

$$m_1 x_1(t) + m_2 x_2(t) + m_3 x_3(t) = 0, \quad (24)$$

and the conserved momentum gives

$$m_1 v y_1(t) + m_2 v y_2(t) + m_3 v y_3(t) = 0. \quad (25)$$

So the dynamics of the TBS system with the tree objects in their aphelion or perihelion are obtained by specifying four values.

The TBS system with the ellipses in Figure 1, used in the present investigations, is started with (mass unit given by  $m_1$  and dynamics units given by the gravitational constant  $G = 1$ ) with

*input* :  $m_1, x_1(0), vy_1(-\delta t/2), m_2, m_3 = 1, -200000, 0.009, 0.5, 100,$

and with the heavy object at the origin and in rest at the start  $vx_3(-\delta t/2) = vy_3(-\delta t/2) = 0$ .

The figures in the article are obtained by the discrete algorithm with  $\delta t=100$ . The result with regular dynamics, shown in the figures is not sensitive to  $\delta t$ .

- 
- [1] Springel, V.: High Performance Computing and Numerical Modelling, Star Formation in Galaxy Evolution: Connecting Numerical Models to Reality, Springer, New York, (2016) 251
  - [2] Vogelsberger, M., Marinacci, F., Torrey, P., Puchwein, E.: Cosmological Simulations of Galaxy Formation, Nat. Rev. Phys. **2**, 42-66 (2020)
  - [3] Hockney, R. W., Goel, S. P., Eastwood, J. W.: Quit High-Resolution Computer Models of a Plasma, J. Comput. Phys. **14**, 148-158 (1974)

- [4] Efsthathiou, G., Davis, M., Frenk, C. S., White, D. M.: Numerical Techniques for Large Cosmological  $N$ -Body Simulations, *ApJS* **57**, 241-260 (1985)
- [5] Bagla, J. S.: TreePM: A Code for Cosmological  $N$ -Body Simulations, *J. Astrophys. Astr.* **23**, 185-196 (2002)
- [6] Toxvaerd, S.: Testing the approximations in large-scale simulations of systems with gravitational forces, *J. Chem. Phys.* **163**, 084101 (2025)
- [7] I. Newton, PHILOSOPHIÆ NATURALIS PRINCIPIA MATHEMATICA. *LONDINI, Anno MDCLXXXVII*
- [8] Šuvakov, M., Dmitrašinović, V.: Three Classes of Newtonian Three-Body Planar Periodic Orbits, *Phys. Rev. Lett.* **110**, 114301 (2013)
- [9] Dmitrašinović, V., Hudomal, A., Shibayama, M., Sugita, A.: Linear stability of periodic three-body orbits with zero angular momentum and topological dependence of Kepler's third law: a numerical test, *J. Phys. A: Math. Theor.* **51**, 315101 (2018)
- [10] Li, X., Tao, Y., Li, X., Liao, S.: A numerical scheme to obtain periodic three-body orbits with finite angular momentum, *New Astronomy* **119**, 102407 (2025)
- [11] Krishnaswami, G., Senapati, H.: An Introduction to Classical Three-Body Problem, *Resonance* **24**, 87-114 (2019)
- [12] Toxvaerd, S.: Discrete Molecular Dynamics, *Comprehensive Computational Chemistry* **3**, Elsevier, 2023, 329-343
- [13] Toxvaerd, S.: Energy, temperature, and heat capacity in discrete classical dynamics, *Phys. Rev E* **109**, 015306 (2024)
- [14] Toxvaerd, S.: Newton's algorithm for discrete classical dynamics, *J. Chem. Phys.* **162**, 024107 (2025)
- [15] Toxvaerd, S.: Newton's discrete dynamics, *Eur. Phys. J. Plus*, **135**:267 (2020)
- [16] Milgrom, M.: A Modification of the Newtonian Dynamics: Implications for Galaxies, *The Astrophysical J.* **270**, 371-383 (1983)
- [17] Gentile, G., Famaey, B., de Blok, W. J. G.: Things about MOND, *A&A*, **527** A76 (2011)
- [18] Toxvaerd, S.: Simulations of galaxies in an expanding Universe with modified Newtonian dynamics (MOND) and with modified gravitational attractions (MOGA), *Eur. Phys. J. Plus* **139**, 395 (2024)
- [19] Toxvaerd, S.: Planetary systems with forces other than gravitational forces, *Celest. Mech.*

- Dyn. **134** :40 (2022)
- [20] Capozziello, S., De Laurentis, M.: Extended Theories of Gravity, Phys. Rep. **509**, 167-321 (2011)
  - [21] Clifton, T., Ferreira, P. G., Padilla, A., Skordis, C.: Modified gravity and cosmology, Phys. Rep. **513**, 1-189 (2012)
  - [22] Capozziello, S., Capriolo, M., Nojiri, S.: Gravitational waves in  $f(Q)$  non-metric gravity via geodesic deviation, Phys. Lett. B **850**, 138510 (2024)
  - [23] Winther, H. A., et al: Modified gravity  $N$ -body code comparison project, MNRAS **454**, 4208-4234 (2015)
  - [24] K. Koyama, K.: Cosmological tests of modified gravity, Rep. Prog. Phys. **79**, 046902 (2016)